First principle calculation of elastic and thermodynamic properties of stishovite*

Liu Xun(刘 勋)[a)b)], Zhou Xian-Ming(周显明)[a)b)†], and Zeng Zhao-Yi(曾召益)[b)]

[a)] *Laboratory for Shockwave and Detonation Physics, Institute of Fluid Physics, China Academy of Engineering Physics, Mianyang* 621900, *China*

[b)] *College of Physical Science and Technology, Sichuan University, Chengdu* 610065, *China*

(Received 1 February 2010; revised manuscript received 7 April 2010)

Using *ab initio* plane-wave pseudo-potential density functional theory method, the elastic constants and band structures of stishovite were calculated. The calculated elastic constants under ambient conditions agree well with previous experimental and theoretical data. C_{13}, C_{33}, C_{44}, and C_{66} increase nearly linearly with pressure while C_{11} and C_{12} show irregularly changes with pressure over 20 GPa. The shear modulus (C_{11}-C_{12})/2 was observed to decrease drastically between 40 GPa and 50 GPa, indicating acoustic mode softening in consistency with the phase transition to $CaCl_2$-type structure around 50 GPa. The calculated band structures show no obvious difference at 0 and 80 GPa, being consistent with the high incompressibility of stishovite. With a quasi-harmonic Debye model, thermodynamic properties of stishovite were also calculated and the results are in good agreement with available experimental data.

Keywords: first principle, elastic constants, thermal properties, quasi-harmonic Debye model

PACC: 7115M, 6220D, 6740K

1. Introduction

The properties of stishovite, i.e. the octahedrally coordinated polymorph of silica in the rutile structure, are of wide interest.[1] Natural stishovite has been observed in meteorites,[2] and its presence in the deep Earth is inferred from associations in diamond inclusions.[3] In the Earth's interior, stishovite is expected to be an important constituent in basaltic compositions and deeply subducted sediments, so it plays an important role in geophysics.[4] It is also one of the hardest oxides, its hardness was claimed to be the secondary to the cotunnite-type TiO_2 synthesized at a high pressure of 60 GPa.[5]

The behaviour of stishovite under high pressure and high temperature has been the subject of many experimental and theoretical studies.[6−9] Stishovite transforms to an orthorhombic $CaCl_2$-type structure around 50 GPa.[10,11] The elastic properties of stishovite were studied previously both in diamond anvil cells[12] and by fit to shock wave data.[13] The bulk modulus K_{0T} and its pressure derivative K'_{0T} assume a wide range of values. K_{0T} ranges from 235 GPa to 347 GPa while K'_{0T} ranges from 1.7 to 6.9 as convened from Ref. [14]. The large discrepancies indicate a need for further studies on the elastic properties of stishovite. Thermodynamic properties play important roles in the high temperature-high pressure equation of state, but determining the thermodynamic properties under extreme conditions with experimental method is difficult. Previous theoretical studies on stishovite using different theories are mainly about its structural,[9] cohesive[15] and phase transition properties,[10] seldom attention has been paid to the elastic and thermodynamic properties. Here, using the first-principle plane-wave pseudo-potential method and a quasi-harmonic Debye model, we carried out a comprehensive study on the elastic, anisotropic, band structural and thermodynamic properties of stishovite.

2. Computational details

In our electronic structure calculations, the ultrasoft pseudo-potentials introduced by D. Vanderbilt were employed for all the ion–electron interactions,[16] together with the local density approximation (LDA) for the exchange–correlation function.[17] A plane-wave basis set with energy cut-off 500 eV was ap-

*Project supported by the Science and Technology Foundation of the China Academy of Engineering Physics (Grant No. 2008B0101001).

†Corresponding author. E-mail: xianming_zhou@caep.ac.cn

© 2010 Chinese Physical Society and IOP Publishing Ltd

plied. Pseudo-atomic calculations were performed for Si $3s^2 3p^2$ and O $2s^2 2p^4$. For the Brillion zone sampling, we used a 6×6×10 Monkhorst–Pack mesh. The self-consistent convergence of the total energy was 10^{-6} eV/atom. A full optimization of the cell structure for each target external pressure was performed by using the Broyden–Fletcher–Goldfarb–Shenno (BFGS) minimization technique.[18] It is found that these parameters are sufficient in leading to well converged total energy, geometrical configurations and elastic stiffness coefficients. All these total energy electronic structure calculations were implemented by the plane-wave pseudo-potential density functional theory using the Cambridge Serial Energy (CASTEP) program.[19,20]

From Hooke's law, the relation of stress and strain tensors can be expressed as

$$\sigma_{ij} = c_{ijkl} e_{kl}. \tag{1}$$

The elastic constants are calculated as the second derivatives of the internal energy with respect to the strain tensor

$$c_{ijkl} = \frac{\partial^2 E}{\partial \varepsilon_{ij} \varepsilon_{kl}}. \tag{2}$$

For tetragonal structured stishovite (space group number: 136), there are six independent non-zero elastic constants: C_{11}, C_{12}, C_{13}, C_{33}, C_{44}, and C_{66}. The bulk modulus B and shear modulus G can be calculated from elastic constants by the following equations:[21,22]

$$B_{\rm V} = (1/9)[2(C_{11} + C_{12}) + C_{33} + 4C_{13}], \tag{3}$$

$$G_{\rm V} = (1/30)(M + 12C_{44} + 12C_{66}), \tag{4}$$

$$B_{\rm R} = C^2/M, \tag{5}$$

$$G_{\rm R} = (5/2)[C^2 C_{44} C_{66}]/[3B_{\rm V} C_{44} C_{66} + C^2(C_{44} + C_{66})], \tag{6}$$

$$B_{\rm VRH} = \frac{B_{\rm V} + B_{\rm R}}{2}, \tag{7}$$

$$G_{\rm VRH} = \frac{G_{\rm V} + G_{\rm R}}{2}, \tag{8}$$

$$M = C_{11} + C_{12} + 2C_{33} - 4C_{13}, \tag{9}$$

$$C^2 = (C_{11} + C_{12})C_{33} - 2C_{13}^2, \tag{10}$$

where V denotes the Voigt bound, R denotes the Reuss bound, and VRH denotes the Voigt–Reuss–Hill average. Poisson's ratio can be defined as

$$\nu = \frac{3B_{\rm VRH} - 2G_{\rm VRH}}{2(3B_{\rm VRH} + G_{\rm VRH})}. \tag{11}$$

The quasi-harmonic Debye model has been widely used to calculate the thermodynamic properties of materials,[23−26] in which the non-equilibrium Gibbs function $G(V; P, T)$ is defined as

$$G(V; P, T) = E(V) + PV + A_{\rm vib}(\theta(V); T), \tag{12}$$

where $E(V)$ is the total energy per unit cell, PV corresponds to the constant hydrostatic compression process, $\theta(V)$ is the Debye temperature, and the vibrational contribution $A_{\rm vib}$ can be written as

$$A_{\rm vib}(\theta; T) = nk_{\rm B}T\left[\frac{9\theta}{8T} + 3\ln(1 - {\rm e}^{-\theta/T}) - D(\theta/T)\right], \tag{13}$$

where $k_{\rm B}$ is the Boltzmann constant, $D(\theta/T)$ represents the Debye integral, n is the number of atoms in each unit. The Debye temperature θ is expressed as

$$\theta = \frac{\hbar}{k_{\rm B}}[6\pi^2 V^{1/2} n]^{1/3} f(\delta)\sqrt{\frac{B_{\rm s}}{M}}, \tag{14}$$

where M is the molecular mass per formula unit, $B_{\rm s}$ is the adiabatic bulk modulus, δ is the Poisson ratio, and $f(\delta)$ is given by

$$f(\delta) = \left\{3\left[2\left(\frac{2}{3}\left(\frac{1+\delta}{1-2\delta}\right)\right)^{3/2} + \left(\frac{1}{3}\left(\frac{1+\delta}{1-\delta}\right)\right)^{3/2}\right]^{-1}\right\}^{1/3}. \tag{15}$$

The constant volume specific heat $C_{\rm v}$, Grüneisen parameter γ and thermal expansion coefficient α can be calculated by the following equations[27,28]

$$C_{\rm v} = 3nk_{\rm B}\left[4D\left(\frac{\theta}{T}\right) - \frac{3\theta/T}{{\rm e}^{\theta/T} - 1}\right], \tag{16}$$

$$\gamma(V) = -\frac{{\rm d}\ln\theta(V)}{{\rm d}\ln V}, \tag{17}$$

$$\alpha = \gamma C_{\rm v}/(B_{\rm T} V), \tag{18}$$

where $B_{\rm T}$ is the isothermal bulk modulus.

3. Results

3.1. Elastic properties

The optimized lattice parameters are a=4.13 and c=2.64, a little smaller than the experimental values of a=4.18 and c=2.66,[9] which is normal because our calculated lattice parameters are the 0 K values, while the experimental values are at 300 K. Otherwise, the LDA method used to give a smaller initial volume.[29] The lattice parameters decrease nearly linearly with pressure as shown in Fig. 1. The experimental results

of Andrault *et al.* were also plotted and are in agreement with our calculated results. The values of linear stiffness, defined as $K_l = -l\mathrm{d}p/\mathrm{d}l$,[30] are also calculated found to be k_{a0}=719 GPa and k_{c0}=1405 GPa at zero pressure. It is more incompressible along c axis than along a axis. This is explained by the stishovite crystal structure in which six-coordinated Si octahedron are edge-shared along c axis and corner-shared along a axis, resulting in strong bonding along c axis.[31]

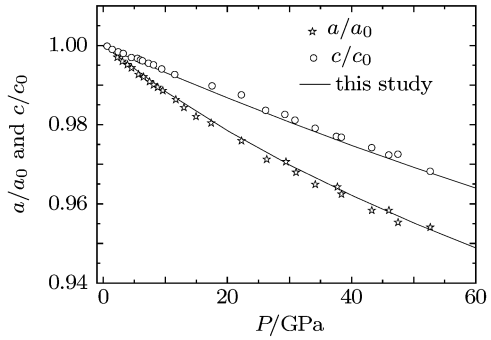


Fig. 1. Variation of a/a_0 and c/c_0 with pressure. Results of this study are compared with the experiment of Andrault *et al.*[32]

The calculated P–V relationship is plotted in Fig. 2 and is in agreement with the latest experimental results.[12,32,33] A fit to the Birch–Murnaghan 3rd-order equation of state gives K_{0T} =305 GPa and $K'_{0\mathrm{T}}$ = 5.0. In Table 1, some previous results are listed. Obvious discrepancies can be seen. One reason is that stoshovite is highly uncompressible and thus sensitive to non-hydrostatic stress, another reason may be that different equations of state are used and different pressure ranges are fitted. Our calculated results agrees very well with the experimental value of Shieh *et al.* (2002),[1] Luo *et al.* (2003),[13] and Li *et al.* (1996).[34] The results calculated by Cohen using LAPW method are not so accurate, which have a larger $K_{0\mathrm{T}}$ and a smaller $K'_{0\mathrm{T}}$.[35]

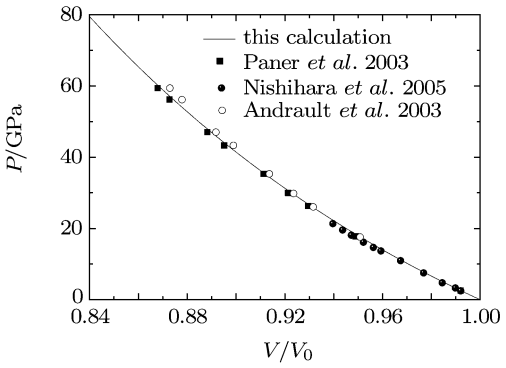


Fig. 2. The P–V data for stishovite with volume normalized to the zero-pressure value. Results of this study are compared with the latest experimental results.

Table 1. Bulk modulus $K_{0\mathrm{T}}$ and its pressure derivative $K'_{0\mathrm{T}}$.

method	$K_{0\mathrm{T}}$/GPa	$K'_{0\mathrm{T}}$	$P_{\max}$/GPa	medium	reference
Brillion	299(1)	4.4(2)	12	MEW[a]	[31]
	310(3)		Ambient		[36]
XRD	304[b]	4.6(1)	60		[1]
	292(13)	6[b]	29	MEW, Ar	[37]
	310(1)	4.6(2)	128	MEW, NaCl	[32]
	312.9(34)	4.8(2)	59	Annealing	[12]
	297(5)	4.3(4)	22	NaCl	[33]
shock data	306(5)	5.0(2)	235		[5]
ultrasonic	305(5)	5.3(1)	3		[34]
calculated	324	4.04	150		[35]
	305	5	80		this study

a. MEW: methanol-ethanol-water mixture, b. fixed value. $P_{\max}$ is the highest pressure reached in corresponding experiment or calculation. Numbers in round brackets are uncertainties.

The calculated elastic constants were listed in Table 2 and are compared with some previous experimental and theoretical results, the agreement is obviously good. Compared with the latest experimental results of Jiang *et al.*, the change ratios of C_{11}, C_{33}, C_{12}, C_{13}, C_{44} and C_{66} are 3.7%, 1.6%, 1.0%, 2.1%, 1.6% and 1.6%, respectively. With Eq. (3) to Eq. (10), the bulk and shear moduli were calculated to be B_{VRH}=304.0 GPa, G_{VRH}=233.5 GPa, and the Poisson's ratio of 0.194 calculated from Eq. (11) is close to the value of 0.202 calculated by Ottonello *et al.*[14] With increasing pressure, the elastic constants increase nearly linearity except C_{11} and C_{12} which show irregularly changes over 20 GPa as shown in Figs. 3 and 4. The shear modulus $(C_{11} - C_{12})/2$ was observed to reduce drastically between 40 GPa and 50 GPa, indicating acoustic mode

softening and being consistent with the phase transition to $CaCl_2$-type structure around 50 GPa. Stishovite shows strong elastic anisotropy. C_{33} is the largest among all individual constants and is about 1.7 times the value of C_{11}.

Table 2. Elastic moduli for stishovite.

	elastic constants (in GPa)					
	C_{11}	C_{33}	C_{12}	C_{13}	C_{44}	C_{66}
this study	472	750	197	188	262	326
Ref. [31][a]	455(1)	762(1)	199(1)	192(1)	258(1)	321(1)
Ref. [36][a]	466(3)	775(4)	207(8)	204(4)	258(2)	310(6)
Ref. [38][b]	462	734	210	195	255	324
Ref. [39][b]	480	735	245	220	260	340

a. Experimental results, b. calculated results. Numbers in round brackets are uncertainties.

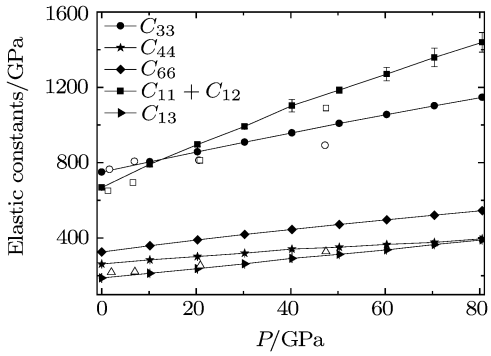


Fig. 3. Change of elastic constants with pressure. Open circles, squares and triangles show C_{33}, $(C_{11}+C_{12})$, and C_{13} calculated by Cohen using LAPW method respectively.

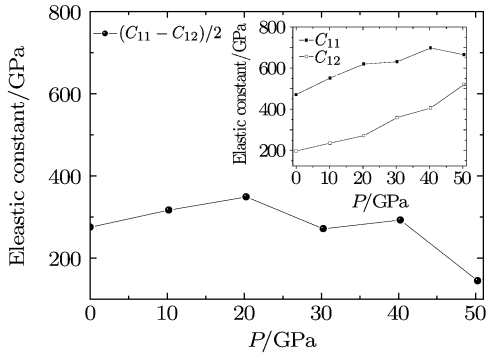


Fig. 4. Change of shear modulus with pressure.

3.2. Band structure

Figure 5 shows calculated band structures for stishovite at 0 and 80 GPa, respectively. No conspicuous change was found except the widening of the bands, which is consistent with the high incompressibility of stishovite. The valence band consists primarily of O 2p states and is quite wide, but the dispersion of individual bands in the manifold is quite small. As specified by Cohen,[35] the small dispersion implies a localized ionic or atomic character, but the very large band width implies strong covalency, so that the mixed ionic-covalent character is evident in stishovite band structure. The band width of O 2p and 2s states at 0 GPa are 11.2 eV and 4.3 eV,

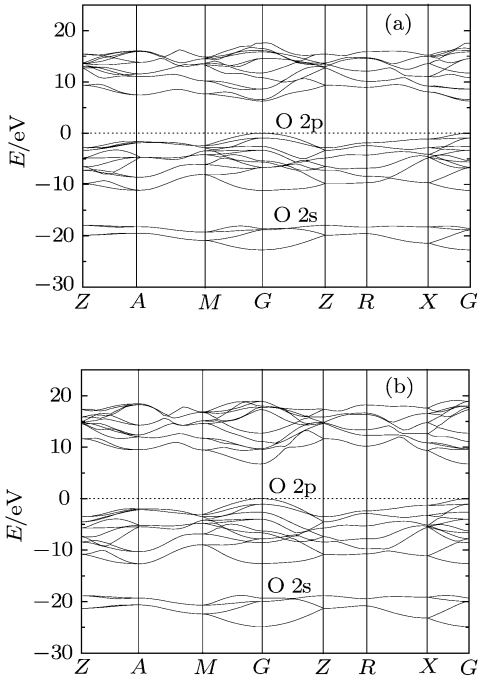


Fig. 5. The band structure at different pressures: (a) 0 GPa and (b) 80 GPa.

respectively, the gap between O 2s and 2p states is 7.3 eV. These values agree well with Cohen's calculation which gave an O 2s band of 11.2 eV and an O 2p band of 4.4 eV, with a gap of 7.0 eV. At 80 GPa, the band widths of O 2s and 2p states are 12.6 eV and 5.5 eV, respectively, and the gap between them decreases to 6.7 eV. The band gap of stishovite increases from 6.3 eV at 0 GPa to 6.7 eV at 80 GPa, unlike most of materials whose band gap decreases under external pressure. The band gap also increases with pressure in

diamond, Fahey *et al.* explained the positive pressure derivative of the diamond band gap by the absence of d-states with the same principal quantum number as the upper valence states,[40] and Cohen considered this may also hold for stishovite.[35]

3.3. Thermodynamic properties

With the quasi-harmonic Debye model, the thermodynamic properties of stishovite were calculated. In Fig. 6, the dependences of calculated normalized volume V/V_0 on pressure P at a given temperature are shown. The diamonds are Nishihara *et al.*'s x-ray diffraction results. The agreement is excellent. In Fig. 7, the dependence of normalized volume on temperature at zero pressure is shown. At low temperature, our calculated results agree well with Ito *et al.*[41] and Nishihara *et al.*'s experimental results.[33] With temperature growing to above 1100 K, the discrepancy appears. This may be due to the high temperature, at which the experimental uncertainty becomes big.

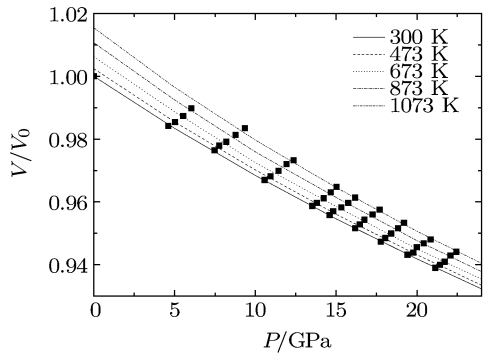


Fig. 6. The P–V data for stishovite, with volume normalized to the zero-pressure value at different temperatures. Diamonds are Nishihara *et al.*'s x-ray diffraction experimental results.

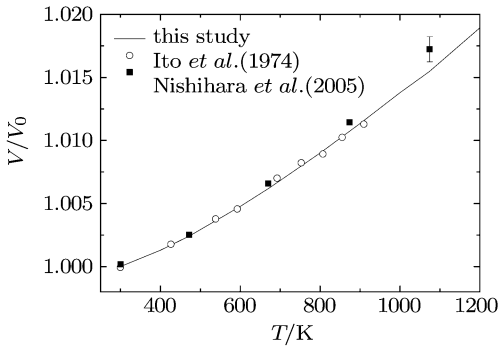


Fig. 7. Normalized volume (V/V_0) of stishovite at zero pressure as a function of temperature.

At constant pressure, the thermal expansion coefficient increases with temperature as shown in Fig. 8. Our calculated values of thermal expansion coefficient at zero pressure and 300 K agree well with Darashev *et al.*'s experimental result[42] and close to Weaver at al's experimental result,[43] but far from Endo *et al.*[44] and Ito *et al.*'s experimental results.[41] At higher temperature, our result is close to Ito *et al.*'s and Hofmaister *et al.*'s experimental results.[45] At constant temperature, the thermal expansion coefficient decreases with pressure. In Fig. 8, Suito *et al.*'s experimental results at 10.5 GPa are shown,[46] the experimental results are obviously smaller than our calculated thermal expansion coefficient at 10 GPa.

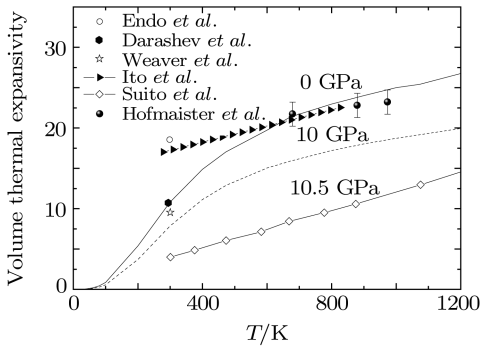


Fig. 8. Calculated thermal expansion coefficient at constant pressures. Solid line and dashed line are calculated thermal expansion coefficient at 0 and 10 GPa, respectively.

The calculated constant volume specific heat increases with temperature and tends to $3nR$ at high temperature. The constant pressure specific heat C_p can be calculated from C_v by the following equation

$$C_\mathrm{p} = C_\mathrm{v}(1 + \alpha\gamma T). \tag{19}$$

The calculated C_p agrees well with the results calculated by Nishihara *et al.*[29]as shown in Fig. 9.

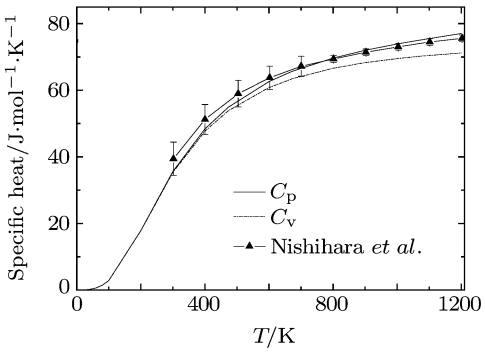


Fig. 9. Calculated specific heat at zero pressure.

4. Summary

In summary, the elastic properties, band structure and thermal properties of stishovite have been

extensively studied by using pseudo-potential plane wave method together with a quasi-harmonic Debye model. Sthishovite shows strong anisotropy, it is more incompressible along c axis than along a axis. The calculated elastic constants under ambient conditions agree well with previous experimental and theoretical data. C_{13}, C_{33}, C_{44}, and C_{66} increase nearly linearly with pressure while C_{11} and C_{12} show irregular changes with pressure over 20 GPa, the shear modulus $(C_{11}-C_{12})/2$ was observed to decrease drastically between 40 GPa and 50 GPa, indicating acoustic mode softening and is consistent with the phase transition to $CaCl_2$-type structure around 50 GPa. The calculated band structure shows no obvious difference at 0 and 80 GPa, begin consistent with the high incompressibility of stishovite. The band gap decreases with pressure, which is consistent with Cohen's LAPW calculation. Our calculated compression curves at evaluated temperatures and pressures agree well with available experimental data. The thermal expansion coefficient and specific heat were also calculated and are in agreement with the experimental results, showing the applicability of quasi-harmonic Debye model in calculating the thermal properties of stishovite.

References

[1] Shieh Sean R, Duffy Thomas S and Li Baosheng 2002 *Phys. Rev. Lett.* **89** 255507
[2] Goresy A E, Dubrovinsky L, Sharp T G, Saxena S K and Chen M 2000 *Science* **288** 1632
[3] Joswig W, Stachel T, Harris J, Baur W and Brey G 1999 *Earth Planet. Sci. Lett.* **173** 1
[4] Shieh Sean R, Duffy Thomas S and Shen Guoyin 2005 *Earth Planet. Sci. Lett.* **235** 273
[5] Luo Sheng-Nian, Swadener J G, Ma Chi and Tschauner Oliver 2007 *Physica* B **399** 138
[6] Tschauner Oliver, Luo Sheng-Nian, Asimow Paul D and Ahrens Thomas J 2006 *Am. Mineral.* **91** 1857
[7] Grimsditch M, Popova S, Brazhkin V V and Voloshin R N 1994 *Phys. Rev.* B **50** 12984
[8] Rudra Jayanta Kumar and Fowler W Beall 1983 *Phys. Rev.* B **28** 1061
[9] Keskar Nitin R, Troullier N, Martins José Luís and Chelikowsky James R 1991 *Phys. Rev.* B **44** 4081
[10] Karki B B, Warren M C, Stixrude L, Ackland G J and Crain J 1997 *Phys. Rev.* B **55** 3465
[11] Akins Joseph A and Ahrens Thomas J 2002 *J. Geophys. Lett.* **29** 101394
[12] Panero Wendy R, Benedetti Laura Robin and Jeanloz Raymond 2003 *J. Geophys. Res.* **108** (B1) 2015
[13] Luo Sheng-Nian, Mosenfelder J L, Asimow P D and Ahrens Thomas J 2002 *J. Geophys. Lett.* **29** 1691
[14] Ottonello G, Zuccolini M Vetuschi and Civalleri B 2009 *Calphad.* **33** 457
[15] Lee Changyol 1996 *Phys. Rev.* B **54** 8973
[16] Vanderbilt D 1990 *Phys. Rev.* B **41** 7892
[17] Gerperley D M and Alder B J 1980 *Phys. Rev. Lett.* **45** 566
[18] Pfrommer B G, Ĉoté M, Louie S G and Cohen M L 1997 *J. Comp. Physiol.* **131** 233
[19] Payne M C, Teter M P, Allen D C, Arias T A and Joannopoulos J D 1992 *Rev. Mod. Phys.* **64** 1045
[20] Milman V, Winkler B, White J A, Packard C J, Payne M C, Akhmatskaya E V and Nobes R H 2000 *Int. J. Quantum Chem.* **77** 895
[21] Wu Z J, Zhao E J, Xiang H P, Hao X F, Liu X J and Meng J 2007 *Phys. Rev.* B **76** 054115
[22] Zhu J, Yu J X, Wang Y J, Chen X R and Jing F Q 2008 *Chin. Phys.* B **17** 2216
[23] Li X F, Peng W M, Shen X M, Ji G F and Zhao F 2009 *Acta Phys. Sin.* **58** 2660 (in Chinese)
[24] Yu J X, Fu M, Ji G F and Chen X R 2009 *Chin. Phys.* B **18** 269
[25] Chen D, Chen J D, Zhao L H, Wang C L, Yu B H and Shi D H 2009 *Chin. Phys.* B **18** 738
[26] Xu G L, Chen J D, Chen D, Ma J Z, Yu B H and Shi D H 2009 *Chin. Phys.* B **18** 744
[27] Zhang W, Cheng Y, Zhu J and Chen X R 2009 *Chin. Phys.* B **18** 1207
[28] Blanco M A, Francisco E and Luaña V 2004 *Comput. Phys. Commun.* **57** 157
[29] Dewhurst J K, Lowther J E and Madzwara L T 1997 *Phys. Rev.* B **55** 11003,
[30] Hubertus Giefers and Felix Porsch 2007 *Physica* B **400** 53
[31] Jiang F M, Gwanmesia G D, Dyuzheva T I and Duffy T S 2009 *Phys. Earth Planet. Inter.* **172** 235
[32] Andrault D, Angel R J, Mosenfelder J L and Bihan T Le 2003 *Am. Mineral.* **88** 301
[33] Yu Nishihara, Keisuke Nakayama, Eiichi Takahashi, Tomohiro Iguchi and Ken-ìchi Funakoshi 2005 *Phys. Chem. Mine.* **31** 660
[34] Li B S, Rigden S M and Liebermann R C 1996 *Phys. Earth Planet. Inter.* **96** 113
[35] Cohen Ronald E 1991 *Am. Mineral.* **76** 733
[36] Brazhkin V V, McNeil L E, Grimsditch M, Bendeliani N A, Dyuzheva T I and Lityagina L M 2005 *J. Phys.*: *Condense Matter* **17** 1869
[37] Yamanaka T, Fukuda T and Tsuchiya J 2002 *Phys. Chem. Miner.* **29** 633
[38] Karki B B, Stixrude L and Crain J 1997 *Geophys. Res. Lett.* **24** 3269
[39] Bengt Holm and Rajeev Ahuja 1999 *J. Chem. Phys.* **111** 2071
[40] Fahey S, Chang K J, Louis S G and Cohen M L 1987 *Phys. Rev.* B **35** 5856
[41] Ito H, Kawada K and Akimoto S 1974 *Phys. Earth Planet. Inter.* **8** 277
[42] Doroshev A M, Galkin V M and Kuznesov G N 1988 *Geochem. Int.* **25** 92
[43] Weaver J S, Takahashi T and Bassett W A 1973 *Trans. Am. Geophys. Union* **54** 475
[44] Endo S, Aki T, Akahama Y, Wakatsuki M, Nakamura T, Tomii Y, Koto K, Ito Y and Tokonami M 1986 *Phys. Chem. Miner.* **13** 146
[45] Kieffer S W 1979 *Rev. Geophys. Space Phys.* **17** 1
[46] Kaichi Suito, Makoto Miyoshi, Akifumi Onodera, Osamu Shimomura and Takumi Kikegawa 1996 *Phys. Earth Planet. Inter.* **93** 215